# Retro-VLP: Towards Single Light Source-based Real-time Indoor Positioning

Mahmoud Nazzal\*, Ahmed Sawalmeh<sup>‡ §</sup>, Sihua Shao<sup>¶</sup>,
Muhammad Anan<sup>||</sup>, Abdallah Khreishah\*, and Ali Alanazi<sup>‡§</sup>

\* New Jersey Institute of Technology, Newark, NJ 07102, USA

<sup>‡</sup> Northern Border University, Arar 73222, Saudi Arabia

§ Remote Sensing Unit, Northern Border University, Arar, Saudi Arabia

New Mexico Tech, Socorro, NM 87801, USA

|| Alfaisal University, Riyadh 11533, Saudi Arabia

E-mails: mahmoud.nazzal@ieee.org, ahmad.sawalmeh@nbu.edu.sa, sihua.shao@nmt.edu, manan@alfaisal.edu, abdallah@njit.edu, ali.hamdan@nbu.edu.sa

Abstract-Due to the increasing usage of Internet-ofthings (IoT) devices, their positioning is an essential need in many real-world applications. Along this line, visible light communication (VLC) is a principal approach due to its advantages of high accuracy, low computation cost, ubiquitous lighting infrastructure, and being free of RF interference. Still, there is a growing need for improving the positioning accuracy and speed. This paper proposes and prototypes a VLC-based positioning solution using retroreflectors mounted on the IoT devices of interest. The proposed method exploits the retro-reflected power received at several PDs for rendering the coordinates of reflectors in the real world. Specifically, the relative relationships between the magnitudes of reflected light ray power are used to figure out the x-y coordinates such that the centroid of power magnitudes is regarded as the x-y coordinate. Besides, the variance of those magnitudes is used to infer the height of the retroflector (the z-coordinate). The proposed solution excels in its simplicity and fast computation and alleviates the need for sensory devices and active operation. This is validated over executive experiments conducted on a prototype in a real-world environment.

Index Terms—VLC, positioning, localization, retrorefelctors, IoT

## I. INTRODUCTION

Since many Internet-of-Things (IoT) devices are mainly used in indoor environments, their indoor positioning (localization) is of increasing importance both in-home and industrial environments. Positioning is needed in warehouse workspace, airports, and shopping centers to name a few examples. A direct positioning approach is the global positioning system (GPS). However, it is unsuitable for indoor environments and does require expensive communication and hardware overheads on the devices of interest. A better alternative is the visible light communication (VLC)-based approach [1]. The main idea behind this approach is to project light from a source into the object of interest and then to exploit information extracted

from the signal reflected back from the object of interest for its positioning. Such information includes strength, angle-of-arrival, polarization, and light distribution patterns. Based on what information is retrieved and the way how it is used in positioning, there is a variety of VLC-based positioning approaches. The technology of visible light positioning (VLP) describes the functionality of indoor positioning by the means of visible light emitted from the luminaires of the obligatory room lighting and the acquisition of the emitted light at a receiver unit equipped with one or multiple photosensitive devices [2]. Visible Light Sensing (VLS) expands the functionality of visible light into the domain of sensing and detection [3]. The applications that are treatable by means of VLS are manifold and range from simple pose detection [4], occupancy or presence detection [5] to gesture recognition [6], amongst many more. In VLS, the object of desire reflects the light emitted from the light source back towards the receiving element. By placing reflective materials or other components (e.g. an LCD shutter) that modulate the spectrum and/or the intensity of the reflected light, information can be conveyed.

The VLC-based approach possesses several attractive advantages over other solutions. First, is requiring minimal [7] or even no additional hardware complexity [8]. Second, is the minimized interference in the VLC domain due to its LOS nature promising for very fine-grained positioning accuracy levels [9]. Moreover, some recent positioning approaches achieve cm-level accuracy in a real-time operation [10]. Also, the usefulness of the VLC approach is more strongly pronounced with the widespread use of light-emitting diodes (LEDs) for illumination in home, office, and industrial environments.

Despite the clear advantages of the VLC-based approach, it still faces a few challenges. First, is

the non-convex nature of positioning when viewed as an optimization problem. This awes to the nonlinear relationships between the coordinates of an object and the characteristics of its VLC received signals. This forms a barrier against treating positioning as a standard optimization problem [11] as this solution framework tends to give local optima. Besides, signals received from the device of interest depend on both its location and orientation which is another unknown to the positioning problem.

### Motivation and related work

Non-VLP approaches include RF-based methods. Along this line, FRID, Bluetooth, and WiFi [12] solutions exist. However, their positioning accuracy is about 1 m. Ultra-wideband (UWB)-based positioning can achieve location precision within tens of centimeters. Nevertheless, they suffer from the disadvantages of the high hardware cost, short battery lifetime, and lack of interaction with the current devices.

Conventional VLP approaches are based on exploiting the geometric relationship between the device of interest and a strong light source [13]. Despite their simplicity, those approaches require some knowledge of the device of interest, such as partial or full orientation information, a known UE height, or perfect alignment between the transmitter and receiver (UE) orientation directions [11]. Another category of VLP approaches is the optimization-based approach. In this setting, the positioning problem is cast as a standard optimization formulation where the objective is to optimize the positioning accuracy. Attempts along this line include using gradient descent, linear search, and Newton method [14]. This approach alleviates the need for prior knowledge of the object of interest as required by conventional methods. However, the non-convex nature of the problem restricts the outcome to local optima. This makes this approach susceptible to poor positioning performances subject to the quality of the local solution obtained. A third category is based on sparse coding, where the sparsity of the solution is exploited to guide the optimization search. However, there are challenges related to extracting the correct sparsity of the solution. This requires both using the exact sparsity degree and identifying the actual domain where the solution is sparse. Those two requirements are nontrivial and require more investigation for this approach to be effective in diverse operational circumstances.

A recent work, referred to as RETRO [10] sets up the real-time backward channel by using an LCD shutter to modulate the retroreflected light from a corner-cube retroreflector, which distinguishes the retroreflected optical signals from the environmental reflection and the signals retroreflected from other IoT devices. IoT devices can be identified using LCD shutters of distinct

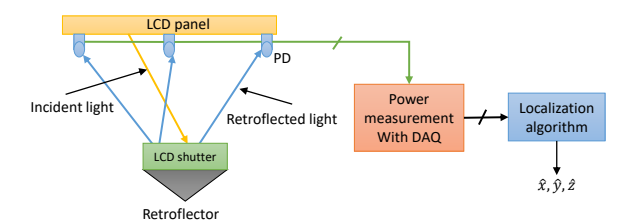


Fig. 1: The system model assumed.

operating frequencies in this setting. Performancewise, RETRO achieves cm-level accuracy, precision, and real-time operation. Retro is based on explicitly solving the coordinates of the retroflector, a small device capable of reflecting VLC light to its source with minimal scattering, minimizing the error in the estimation of received power. An extension of RETRO is PassiveRETRO [15], where retroflectors are completely passive.

Another line of research [16], considers using off-the-shelf retro-reflective foils for VLC-based positioning. This is based on the idea that light impinges on the retroreflective foils towards a photosensitive device collocated in close vicinity to the light source. Along this line, [17] achieves high positioning accuracy at the cost of high computational complexity and excessive memory requirements. Subsequently, [16], [18], indicate that the supervised ML approach of random forest well-suits the VLC positioning problem while offering significant gains in computational complexity and memory requirements.

# **Contributions and Organization**

In summary, we make the following contributions:

- Associating the relationships between retroflected power to guide on the x-y coordinates: in power sensed at a few photodiodes (PD)s are used quantified and used to estimate the x-y coordinates of the retroflector.
- Associating the standard deviation in power magnitudes to the height: This association is used to estimate the height from the standard deviation of the magnitudes of received power values.

Organization: The remainder of this paper is organized as follows. Section II presents the system model and revises preliminaries. The proposed positioning algorithm is presented in Section III. Section IV details the prototyping and experimentation of a proof of concept of the proposed algorithm, with the conclusions in Section V.

#### II. SYSTEM MODEL AND PRELIMINARIES

We use a system model similar to the one in [10]. As shown in Fig. 1, the goal is obtain estimates of the coordinates of the retroflector  $\hat{x}, \hat{y}$ , and  $\hat{z}$ . This model is composed of the following components. First is an

LED panel acting as a (strong) light source. The second is a retroflector circuit composed of a retroflector covered by an LCD shutter with a controlled frequency. This shutter allows or rejects light passage by operating in opaque and transparent states at that frequency. Thus, the retro-reflector reflects the incident ray in a parallel reflected ray, which is then received by the PD. However, one needs to measure this waveform at the specific shutter frequency. This way, one can afford to localize multiple devices simultaneously. To this end, the device's location governs the power received by the PDs. Thus, the correspondence between the location and the power can be exploited to estimate the coordinates of the position. Those PDs are placed to uniformly sample the LCD panel as pictorially represented in Fig. 2.

#### III. THE PROPOSED ALGORITHM

## A. Estimating the x-y coordinates

In essence, the magnitude of received PD power directly correlates with how close the retroflector is. To validate this assumption, Fig. 3 shows the power received by the five PDs as the retroflector is directly placed at 100 cms below PD1. The power received at PD1 is the largest amongst others. This signifies a clear association between the x-y coordinates of the retroflector's position and the relative relationships between the PD power. Thus, we propose considering the magnitude of power as five variables and obtaining the x-y coordinates of the retroflector as the centroid of those variables. Specifically, let us consider the power magnitudes as vector quantities each placed at the position of its underlying PD. Then, we find the centroid of those quantities. So, the x-y coordinates of the retroflector are those of the centroid point.

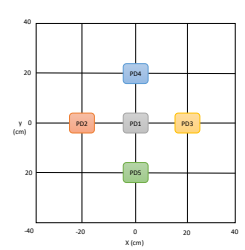


Fig. 2: A top view of the PD layout.

## B. Estimating the z-coordinate

As discussed earlier, there is a direct relationship between the proximity of the retroflect to the PDs and their received power. To this end, we can relate the z-coordinate of the retroflector to those power values. To achieve this mapping, let us consider how different the PDs perceive the retroflector at varying heights (z-coordinates). For this purpose, the following

experiment is conducted. We vary the z-coordinate of the distance between the retroflector and the center of the PD array from 10 cm to 180 cm. For each value, we measure the five PD power magnitudes and calculate their standard deviation. Fig. 4 shows a semi-log plot of the standard deviation in power versus z distance. As seen in this figure, there is an almost linear relationship between the z-distance and the standard deviation in received powers. Exploiting this relationship unleashes a direct association between the two quantities. Therefore, we obtain the z-coordinate based on the magnitude of the standard deviation in power values measured by the five PDs. This experiment empirically verifies the power standard deviation-retroflector's height association in the following lemma.

Let us define a power magnitude vector  $v = [P_i]$ , where i denotes the PD index. To this end, we calculate the standard deviation of this vector as:

$$std(a) = \sqrt{\frac{1}{n} \sum_{i=n}^{n} (a(i) - \bar{a})^2}.$$
 (1)

**Lemma 1:** the standard deviation of the PD power vector is inverse proportional to the height-squared. For the proof, see Appendix.

The main steps of the proposed association-based positioning algorithm are outlined in Algorithm 1.

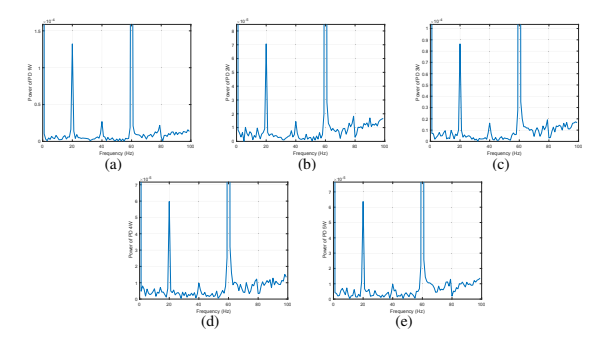


Fig. 3: Spectra of power received by PD1 through PD5 in (a) through (e), respectively, with the retroflector placed at 100 cm underneath PD1.

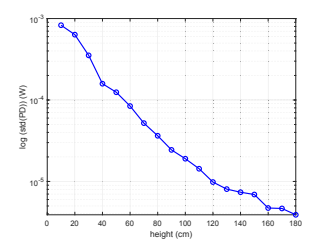


Fig. 4: PD received power standard deviation versus height.

## Algorithm 1 The proposed positioning algorithm.

**Input:** power at the PDs  $P_i, i \in 1, n$ , and a set of known std(v)-height associations.

**Output:** Estimated coordinates of the retroflector's position.

- 1: Assign the values of the power magnitudes  $P_i$  to their location on the PD array
- 2: Calculate the centred of power magnitudes c.
- 3: Set  $\hat{x} \leftarrow c(x)$ .
- 4: Set  $\hat{y} \leftarrow c(y)$ .
- 5: Set  $a = \{P_i\}$
- 6: Calculate the standard deviation of std(a).
- set <sup>2</sup> ← a value fit to the std(v)-height associations.
- 8: **return**  $\hat{x}, \hat{y}, \hat{z}$

#### IV. SETUP AND EXPERIMENTAL VALIDATION

## A. Test bed and setup

A testbed is constructed according to the system model specified in Section II. A photo of this testbed is shown in Fig. 5. The retroflector is mounted on a tripod for keeping track of its position's coordinates in the physical world. As a light source, we use a commercial flat LED panel with evenly distributed light (400W, 4000K, 3770 Lumens) provided by Hyperikon. The PD used in this paper is Hamamatsu S6968 [19]. We operate each PD in the photoconductive mode. The circular retroflectorPS976 (uncoated) is manufactured by Thorlabs [20]. Specifically, each PD is serialized with a 6.8 k $\Omega$  resistor, and the series combination is reversebiased by a 10 V DC voltage. The power received by a PD is proportional to the resistor voltage. We measure this voltage using the Measurement Computing USB-1608FS-Plus Series data acquisition (DAQ) device [21]. This device gives a mealtime measurement of the voltages corresponding to the powers of the five PDs at a sampling frequency of 50K samples/sec. Those measurements are then fed to a PD through the USB port. Next, we record power measurement through MatLab and then apply a fast Fourier transform (FFT) on those power values to extract the actual power magnitude at the LCD shutter's switching frequency. Sample FFT power spectra are shown in Fig. 3. As seen in this figure, each spectrum has two main peaks; one at a 60 Hz frequency as the light source operates at a mains frequency of 60 Hz, and another smaller peak at 20 Hz due to the power reflected by the retroflector. Besides, there are a few other negligibly small peaks due to ambient and measurement noises.

DC power is supplied by a standard DC power source. Eventually, mealtime positioning is done on MatLab. Table I lists several other system parameter values.

TABLE I: System parameters and specifications.

Item	Value
Refractive index	1.51
No. of PDs	5
PD	S6968
$A_s$	150 mm2
Power sampling frequency	50 KHz
retroflector	Thorlabs PS976
LCD shutter frequency	20 Hz
LCD shutter	Pi-cell



Fig. 5: A photo of the prototypes' testbed.

#### B. Positioning performance evaluation

In this experiment, we present a performance evaluation of the proposed algorithm. The performance metric is the empirical cumulative distribution function (CDF) of the positioning error in the  $x,\,y,\,$  and z-coordinates. Specifically, we place the retroflector at 400 points that sample the working area of the positioning system uniformly. At each of these positions, we obtain an estimate of the coordinates of the retroflector and calculate the absolute error between these estimates and the actual  $x,\,y,\,$  and z-coordinates in the physical world. Once the errors for all the positions are calculated, we plot an empirical CDF graph of these errors. This procedure is repeated for 3 height values of 100, 130, and 160 cm.

In this experiment, we compare the proposed algorithm to four variants of the ML positioning approach. This ML approach views the positioning problem as a regression problem, i.e., we train a model based on a ground truth set of training data. Each data point is composed of the power magnitudes seen by the five PDs, and the corresponding output is the x, y, and z coordinates. So, we train three regression models, one to predict each coordinate based on the five measurements. Then, during inference time, we feed the measurement vector of five power magnitudes to each model to obtain estimates of x, y, and z. It is worth mentioning that we collect a training set of 900 1200 training data points, and we randomly select 900 for training. Then, for validation, we use another set of measurements.

There is a variety of ways one can implement this ML predictor. In this experiment, we opt to consider the following regression approaches.

• LR: a linear regression model

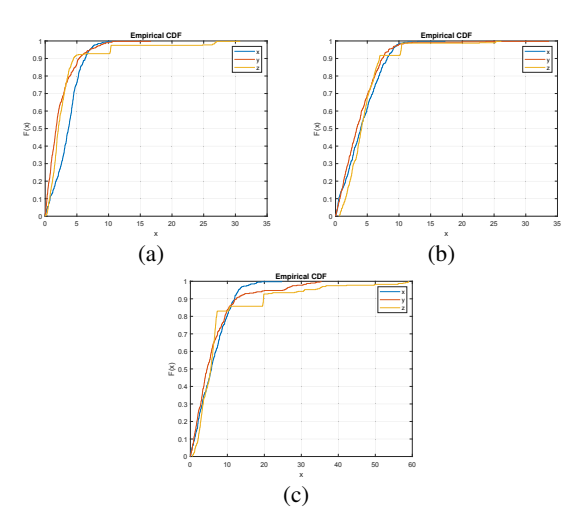


Fig. 6: Empirical CDF positioning error with z = (a) 100 cm, (b) 130 cm, and (c) 160 cm.

- SVM: a support vector machine (SVM) regression model with a Gaussian kernel
- NN: A shallow neural network (NN) regression model
- DMLP: a deep multi-layer perceptron (MLP) regression model with 50 hidden layers and a dropout layer

Fig. 6 shows the empirical CDF plots of the errors in estimating the x, y, and z coordinates of 400 positions uniformly sampling the grid shown in Fig. 2 at three heights from the LED array. Namely, 100, 130, and 160 cm. Correspondingly, the CDF plots of the abovementioned ML-based baselines are shown in Fig. 7. Those figures show that the proposed algorithm has the highest accuracy amongst all methods. This is consistently the same for the x, y, and z coordinates. However, as expected intuitively, the deep MLP approach performs better than the remaining baseline due to its deep nature. However, the four baselines perform poorly in estimating the z-coordinate. This necessitates redefining the ML models to incorporate the height information in their training using specific ML architectures.

To have a rough assessment of the time complexity of the proposed algorithm, we perform positioning 100 times. We measure the execution time for each time, i.e., the time duration from reading the power measurements until producing the coordinate estimates. Fig. 8 shows a CDF plot of the execution time. It is evident that more than 95% of the time, the execution time is less than 0.25 ms. This result assures the proposed algorithm's time complexity and suitability for real-time operation. These results are validated using the tic-toc Matlab command run over Matlab 2021 b operating on an i5-Processor laptop computer

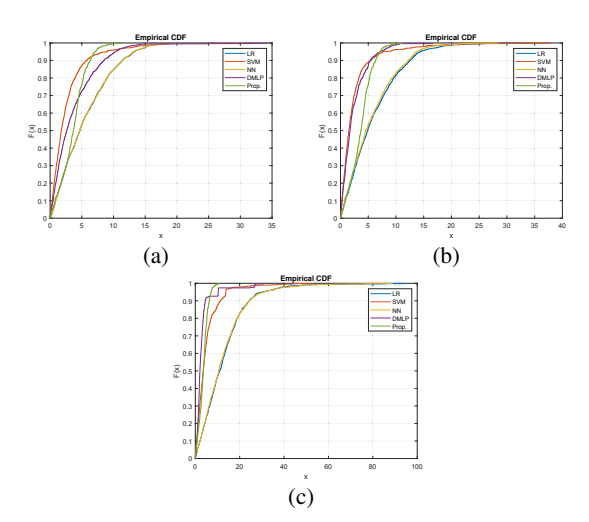


Fig. 7: Empirical CDF positioning error for LR, SVM regression, NN regression, deep MLP regression, and the proposed algorithm for x, y, and z in a through c respectively.

with 8 GBs of RAM.

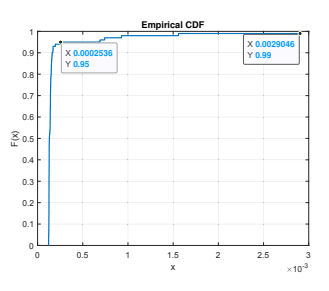


Fig. 8: A CDF plot of execution times for 100 trials.

#### V. CONCLUSIONS

This paper has presented an algorithm for realtime object positioning in an indoor environment. The proposed algorithm is based on exploiting the relative relationships between the power of signals reflected from a retroflector placed on the top of the object to a set of PDs. We have presented a method for associating the relations between the magnitudes of these powers and the *x-y* coordinates and another criterion to associate the standard deviation in those magnitudes to the *z*-coordinate. This work has empirically validated the assumptions behind those associations. Besides, the proposed algorithm achieves an accurate positioning performance with a fast and real-time operation. These findings have been validated through practical experiments conducted over a prototype system.

Interesting future extensions to this work include optimizing the number of PDs to use and their positioning on the LCD array. Besides, the proposed algorithm can be extended to achieve orientation estimation.

#### VI. ACKNOWLEDGMENT

This work is supported by NSF under grant OIA-1757207.

# VII. APPENDIX

**Proof of Lemma 1:** The power received by a PD can be written as follows [10].

$$P_r = P_t \frac{(ml+1)A_s}{8\pi d^2} cos^{ml+1} \theta \alpha \beta, \qquad (2)$$

where  $P_t$  is the transmitted power,  $A_s$  is the effective sensing area of the PD, ml is the Lambertian index,  $\theta$  is the incidence angle to the front face of the retroreflector,  $\alpha$  is the ratio of the effective reflecting area and the maximum effective reflecting area, and  $\beta$  is the ratio of the actual to the virtual effective reflecting area. Also, d is the Euclidean distance between the PD and the retroflector. Thus, we can write  $d^2 = z^2 + v^2$  for an assumed zero elevation and azimuth angles case for simplicity.

To further simplify the analysis, let us refer by q to the quantity  $P_t \frac{(ml+1)A_s}{8\pi} cos^{ml+1} \theta \alpha \beta$  so that we can write  $P_r = q \frac{1}{d^2}$ . To this end, let us consider a power vector of two PDs only, so, a = [P1, P2]. So,  $P1 = q \frac{1}{d^2_1}$ , and  $P2 = q \frac{1}{d^2_2}$ . Also, the mean value of a is  $\bar{a} = q[\frac{1}{d^2_1} + \frac{1}{d^2_2}]$ . So,  $\bar{a} = q \frac{d^2_1 + d^2_2}{d^2_1 d^2_2}$ . Now, let us express the variance of this vector.

$$Var(a) = \frac{1}{2}((P1 - \bar{a})^2 + (P2 - \bar{a})^2), \quad (3)$$

Now, substituting the expression for  $\bar{a}$  into (3),

$$Var(a) = \frac{1}{2}((P1 - q\frac{d_1^2 + d_2^2}{d_1^2 d_2^2})^2 + (P2 - q\frac{d_1^2 + d_2^2}{d_1^2 d_2^2})^2)$$
(4)

Following a few algebraic simplification steps, and considering the specials cases where  $v_1=0$ , i.e.,  $d_1^2=h^2$  we arrive at

$$Var(a) = \frac{1}{2} \frac{q^2}{2} \frac{\left[h^4(-5) - h^2(1 - 6v^2 - v^4)\right]}{h^8 - 2h^6v^2 - h^4v^4}$$
 (5)

Thus, it is evident that Var(a) is inverse proportional to  $h^4$ . Therefore, the standard deviation, i.e., the square root of the variance, is inverse proportional to the height-squared  $h^2$ . This result can be generalized for an a vector corresponding to n PDs.

## REFERENCES

- [1] S. Shao, A. Khreishah, M. Ayyash, M. B. Rahaim, H. Elgala, V. Jungnickel, D. Schulz, T. D. Little, J. Hilt, and R. Freund, "Design and analysis of a visible-light-communication enhanced wifi system," *Journal of Optical Communications* and Networking, vol. 7, no. 10, pp. 960–973, 2015.
- [2] T.-H. Do and M. Yoo, "An in-depth survey of visible light communication based positioning systems," *Sensors*, vol. 16, no. 5, p. 678, 2016.
- [3] Q. Wang and M. Zuniga, "Passive visible light networks: Taxonomy and opportunities," in *Proceedings of the Workshop on Light Up the IoT*, 2020, pp. 42–47.

- [4] A. P. Weiss, S. Z. Rad, and F. P. Wenzl, "Pose detection with backscattered visible light sensing utilizing a single rgb photodiode: A model based feasibility study," in 2020 International Wireless Communications and Mobile Computing (IWCMC). IEEE, 2020, pp. 137–142.
- [5] N. Faulkner, F. Alam, M. Legg, and S. Demidenko, "Watchers on the wall: Passive visible light-based positioning and tracking with embedded light-sensors on the wall," *IEEE Transactions* on *Instrumentation and Measurement*, vol. 69, no. 5, pp. 2522– 2532, 2019.
- [6] E. Lascio, A. Varshney, T. Voigt, and C. Pérez-Penichet, "Poster abstract: Localight-a battery-free passive localization system using visible light," in *Proc. 15th ACM/IEEE Int. Conf. Inf. Process. Sensor Netw.(IPSN)*, 2016, pp. 1–6.
- [7] T. Li, C. An, Z. Tian, A. T. Campbell, and X. Zhou, "Human sensing using visible light communication," in *Proceedings of* the 21st Annual International Conference on Mobile Computing and Networking, 2015, pp. 331–344.
- [8] Z. Zhao, J. Wang, X. Zhao, C. Peng, Q. Guo, and B. Wu, "Navilight: Indoor localization and navigation under arbitrary lights," in *IEEE INFOCOM 2017-IEEE Conference on Com*puter Communications. IEEE, 2017, pp. 1–9.
- [9] Y.-S. Kuo, P. Pannuto, K.-J. Hsiao, and P. Dutta, "Luxapose: Indoor positioning with mobile phones and visible light," in Proceedings of the 20th annual international conference on Mobile computing and networking, 2014, pp. 447–458.
- [10] S. Shao, A. Khreishah, and I. Khalil, "Retro: Retroreflector based visible light indoor localization for real-time tracking of iot devices," in *IEEE INFOCOM 2018-IEEE Conference on Computer Communications*. IEEE, 2018, pp. 1025–1033.
- [11] B. Zhou, A. Liu, and V. Lau, "Visible light-based user position, orientation and channel estimation using self-adaptive location-domain grid sampling," *IEEE Transactions on Wireless Communications*, vol. 19, no. 7, pp. 5025–5039, 2020.
- [12] M. Kotaru, K. Joshi, D. Bharadia, and S. Katti, "Spotfi: Decimeter level localization using wifi," in *Proceedings of the* 2015 ACM Conference on Special Interest Group on Data Communication, 2015, pp. 269–282.
- [13] S.-H. Yang, H.-S. Kim, Y.-H. Son, and S.-K. Han, "Three-dimensional visible light indoor localization using aoa and rss with multiple optical receivers," *Journal of Lightwave Technology*, vol. 32, no. 14, pp. 2480–2485, 2014.
- [14] U. Merzbach, "The mathematical papers of isaac newton," 1971.
- [15] S. Shao, A. Khreishah, and J. Paez, "Passiveretro: Enabling completely passive visible light localization for iot applications," in *IEEE INFOCOM 2019-IEEE Conference on Com*puter Communications. IEEE, 2019, pp. 1540–1548.
- [16] A. P. Weiss and F. P. Wenzl, "Backscattered visible light sensing of retroreflective foils utilizing random forest based classification for speed and movement direction determination and identification of an indoor moving object," in *Telecom*, vol. 2, no. 4. Multidisciplinary Digital Publishing Institute, 2021, pp. 574–599.
- [17] —, "Identification and speed estimation of a moving object in an indoor application based on visible light sensing of retroreflective foils," *Micromachines*, vol. 12, no. 4, p. 439, 2021.
- [18] A. P. Weiss, K. Madane, F. P. Wenzl, and E. Leitgeb, "Random forest based classification of retroreflective foils for visible light sensing of an indoor moving object," in 2021 16th International Conference on Telecommunications (ConTEL). IEEE, 2021, pp. 78–84.
- [19] "Hamamtsu," https://www.hamamatsu.com/resources/pdf/ssd/ s6801etckpin1046e.pdf, accessed: 01-30-2022.
- [20] "Thorlabs," https://www.thorlabs.com/newgrouppage9.cfm? objectgroupid=145, accessed: 01-30-2022.
- [21] "Mc," https://www.mccdaq.com/usb-data-acquisition/USB-1608FS-Plus-Series, accessed: 01-30-2022.